Obrabotka metallov (tekhnologiya, oborudovanie, instrumenty) = Metal Working and Material Science. 2024 vol. 26 no. 1 pp. 155–174
ISSN: 1994-6309 (print) / 2541-819X (online)
DOI: 10.17212/1994-6309-2024-26.1-155-174

NSTU NETI

Obrabotka metallov -
Metal Working and Material Science

Journal homepage: http://journals.nstu.ru/obrabotka_metallov

Semi empirical modeling of cutting temperature and surface roughness in turning of engineering materials with TiAlN coated carbide tool

Nilesh Patil [1, a,*], *Atul Saraf* [2, b], *Atul Kulkarni* [3, c]

[1] Marathwada Institute of Technology, Aurangabad-431010, Maharashtra State, India
[2] National Institute of Technology, Surat, Gujarat 395007, India
[3] Vishwakarma Institute of Information Technology, Survey No. 3/4, Kondhwa (Budruk), Pune – 411048, Maharashtra, India

[a] https://orcid.org/0000-0002-4884-4267, nileshgpatil@rediffmail.com; [b] https://orcid.org/0000-0003-4776-6874, atul.saraf001@gmail.com;
[c] https://orcid.org/0000-0002-6452-6349, atul.kulkarni@viit.ac.in

ARTICLE INFO

Article history:
Received: 20 September 2023
Revised: 31 October 2023
Accepted: 22 January 2024
Available online: 15 March 2024

Keywords:
Semi-empirical model
Regression model
Temperature
Surface roughness

Introduction. In manufacturing, obtaining a given surface roughness of the machined parts is of great importance to fulfill functional requirements. However, the surface roughness significantly affected by the heat generated during the machining process, which can lead to a decrease in dimensional accuracy. The surface roughness significantly affects the fatigue characteristics of the part, and the service life of the cutting tool is determined by the cutting temperature generation. **The purpose of the work.** The purpose of this study is to create semi-empirical models for predicting surface roughness and temperature of various work materials. Enhanced cutting performance is achieved by accurately determining the cutting temperature in the machined zone. However, calculating the cutting temperature for each specific case is fraught with difficulties in terms of labor resources and financial investments. This paper presents a comprehensive empirical formula designed to predict both theoretical temperature and surface roughness. **Methodology**, The performance of the surface roughness and temperature generation was evaluated for the *EN 8*, *Al 380*, *SS 316* and *SAE 8620* materials when processed with *TiAlN*-coated carbide tools. The *TiAlN* coating was obtained by Physical Vapor Deposition (*PVD*) technique. Response surface methodology was used to prepare predictive models. Cutting speed (from 140 to 340 m/min), feed (from 0.08 to 0.24 mm/rev) and depth of cut (from 0.6 to 1 mm) were used as input parameters to measure the characteristics of all materials in terms of surface roughness and cutting temperature. The tool-work thermocouple principle was used to measure the temperature at the chip-tool interface. Novel Calibration Setup was developed to establish the relationship between the Electromotive Force (*EMF*) generated during machining and the cutting temperature. **Results and Discussion.** It is observed that the energy required for mechanical processing was largely converted into heat. The highest cutting temperature is recorded with *SS 316*, followed by *SAE 8620* and *EN 8*. However, low temperature was reported during machining of *Al 380* and it was mainly governed by the thermal conductivity of the material. The lowest surface roughness is observed for *SAE 8620*, *EN 8*, followed by *SS 316* and *Al 380*. The semi-empirical method and regression model equations are in good agreement with each other. Statistical analysis of the nonlinear evaluation reveals that cutting speed, feed rate, and material density have a greater influence on the surface roughness, whereas depth of cut has a greater influence on the temperature change. The study will be very useful for predicting industrial performance when machining *EN 8*, *Al 380*, *SS 316* and *SAE 8620* materials with *TiAlN*-coated carbide tools.

For citation: Patil N.G., Saraf A.R., Kulkarni A.P Semi empirical modeling of cutting temperature and surface roughness in turning of engineering materials with TiAlN coated carbide tool. *Obrabotka metallov (tekhnologiya, oborudovanie, instrumenty) = Metal Working and Material Science*, 2024, vol. 26, no. 1, pp. 155–174. DOI: 10.17212/1994-6309-2024-26.1-155-174. (In Russian).

*** Corresponding author**
Kulkarni Atul P., Ph.D. (Engineering), Professor
Vishwakarma Institute of Information Technology,
Survey No. 3/4, Kondhwa (Budruk),
Pune – 411048, Maharashtra, India
Tel.: 91-2026950419, **e-mail:** atul.kulkarni@viit.ac.in

List of symbols

Symbol	Description
f	Feed (mm)
V_c	Cutting speed (m/min)
doc	Depth of cut (mm)
R_a	Surface roughness (µm)
MRR	Material removal rate (mm^3/rev)
HSM	High speed machining
F_c	Cutting forces (N)
ρ	Density (kg/m^3)
C_p	Specific Heat (J/kg k)
K	Thermal Conductivity(W/mk)
σ	Yield strength (N/m^2)
α	Coefficient of thermal expansion (m/mk)
Θ	Temperature (^oC)
SS 316	Stainless steel ***SS 316***
SAE 8620	Low alloy case hardening steel ***SAE 8620***
EN 8	Engineering steel ***EN 8***
Al 380	Aluminium alloy ***Al 380***
Ø	Buckingham's π theorem constant
$a_1\, a_2\, a_3\, a_4\, a_5$	Power indices
$b_1\, b_2\, b_3\, b_4\, b_5$	Power indices
$M\ L\ T\ \Theta$	Dimensions
CBN	Cubic boron nitride
RSM	Response surface methodology
CCD	Central composite design
ANN	Artificial neural network
LM	Levenberg-Marquardt

Introduction

Surface finish is critical to quality because it directly affects the appearance, functionality, and performance of machined components. Precision machining is essential, especially in aerospace and medical applications where specified surface finish is required to reduce friction, improve wear resistance, or improve corrosion resistance. The influence of surface finish on tribological parameters such as friction and lubrication is crucial to achieve maximum performance and durability. Increased temperatures during machining have a significant impact on tool wear, material integrity and dimensional accuracy. Temperature control is critical for extending tool life and maintaining the structural integrity of machined parts. Predictive modelling optimizes processes by identifying optimal parameters for cost savings through increasing tool life, reducing scrap rates and increasing efficiency. The use of cutting fluid in hard turning is not recommended, since at elevated temperatures when processing materials with a hardness of 48 to 68 HRC, the coolant in the cutting zone begins to boil. This boiling phenomenon promotes thermal deformation, thereby reducing both $\boldsymbol{R_a}$ (surface roughness) and the service life of the cutting tool [1]. In case of machining different materials, its machinability was evaluated using various process parameters such as tool life, material removal rate (*MRR*), cutting force ($\boldsymbol{F_c}$), energy consumption, chip morphology and machined surface roughness ($\boldsymbol{R_a}$). Using high speed machining (*HSM*) while maintaining surface integrity and maintaining tolerance limits requires optimal coordination of factors such as cutting force ($\boldsymbol{F_c}$), process and machine parameters. The right combination of these elements is critical to increasing the efficiency of *HSM* without compromising the quality of the machined surfaces or exceeding specified tolerance limits. This balance ensures that machining can proceed without compromising accuracy and surface quality, contributing to the overall success of high-speed machining operations [2].

Zhao et al., [3] measured the cutting temperature of *Inconel 718* using a two-color infrared thermometer with a ceramic whisker-reinforced tool, and concluded that the large amount of heat generated during machining deteriorates the surface quality of the machined material. Due to the increase in temperature in the cutting zone during machining, the surface quality deteriorated [4]. High tool wear and temperature increase during machining of hardened *AISI 4340* steel can be eliminated using bio-cutting fluid [5]. Post-machining operations are required to improve the surface quality of superalloys, [6]. *Kumar et al.* [7] compared a *RSM* model with an *ANN* model to analyze the turning performance of *AISI D2* steel and concluded that that the *RSM*-based prediction model is more accurate than the *ANN* model for predicting surface quality and cutting temperature. *Gosai* and *Bhavsar* [8] used mathematical models and equations generated by *CCD*-based *RSM* to predict cutting temperature.

The material removal rate during the turning process was higher compared to other traditional machining processes. *Abhang et al.* [9] experimentally measured the temperature of the *EN 31* alloy during turning with tungsten carbide inserts using the natural thermocouple technique. $\boldsymbol{F}$ has a significant effect on the surface roughness: as the $\boldsymbol{f}$ increases, the roughness increases, and as the $\boldsymbol{V_c}$ increases, the roughness decreases [10–12]. *Bhopal et al.* [13] used *RSM* with *CCD* for turning austenized high-strength cast iron with a carbide tool and found that $\boldsymbol{V_c}$ has a more significant effect on surface roughness. *Aouici et al.* [14] used a *CBN* tool for turning *AISI H11* steel, as well as a mathematical model based on *RSM* for ***Ra*** and $\boldsymbol{F_c}$, however, when processing materials reinforced with particles, the surface morphology was changed. *Longbottom and Lanham* [15] conducted a review of temperature measuring devices and found that the measured temperature varied in different places. *Korkut et al.* [16] compared the *ANN* model and the *RA* model and found that the training *ANN* model with the *LM* algorithm demonstrated a higher prediction rate and was useful in measuring the cutting temperature when tested by a qualified *RA* method during machining. *Dhar* and *Kamruzzaman* [17] found that an increase in temperature significantly affects tool wear and surface roughness, and the use of cryogenic cooling gives good results. *Patil* and *Brahmankar* [18] developed a model for surface roughness that takes into account the input parameters, material properties, size of ceramic particles and its volume fraction, and found that the volume fraction and particle size significantly affect the output parameters, as well as that the presence of ceramic particles affects the surface roughness. *Patel* and *Kiran* [19] used a linear regression model to analyze the assessment of the roughness of the surface when processing *AISI 1040* steel. *Patel* and *Gandhi* [20] machined *AISI D2* steel with an *CBN* tool and developed a mathematical model based on the simultaneous action of *f*, V_c and the nose radius, and is in good agreement with the experimental values. But none of them used more than one material for experiments, with the exception of *Rodriguez et al.*, [21] who used *SS 304*, *316L* and *420* materials for turning and developed a model of cutting temperature taking into account thermal conductivity and maximum strength. According to the literature reviewed, the cutting parameters, in particular the cutting speed and feed, have a significant effect on the temperature of the chip-tool contact surface. Various predictive models have been developed, but each model predicted results in a specific parameter range. In addition, several studies have been reported on the effect of *TiAlN* cutting modes and coating parameters on cutting temperature and surface roughness when turning EN 8, Al 380, SS 316 and SAE 8620 materials. In this work, the simplest and most economical method for measuring temperature is developed, involving the use of a tool-work thermocouple. Further, response surface models were developed for the cutting temperature and roughness of these materials, the influence of technological parameters and thermal and physical properties of the materials of the processed parts on the response parameters are studied, and a semi-empirical model is developed to predict the cutting temperature and surface roughness.

Materials and methods

The experimental results were obtained on a *CNC* lathe machine. V_c, ***f*** and ***doc*** were the three adjustable factors in turning operation. In the present work, workpieces made of four materials were used, namely mild steel (*EN 8*) with a diameter of 75 mm, aluminum alloy (*Al 380*) with a diameter of 50 mm, stainless steel (*SS 316*) with a diameter of 75 mm and low alloy steel (*SAE 8620*) with a diameter of 75 mm. The length of each workpiece was 300 mm and each of it was machined. To determine the chemical composition of the above materials, spectroscopic analysis was carried out, the results of which are presented in Table 1. Since the literature indicates that *TiAlN*-coated carbide tools have minimal R_a and tool wear, *Sandvik PVD* (*TiAlN*) coated carbide inserts *CNMG-120408 MS PR1310* (0.8 mm nose radius) with eight cutting edges were used in this work for 20 tests under dry conditions. The contact point between the tool and the workpiece was hot during machining, while the carbon brush touching the workpiece remained cold. The workpiece was mounted in a three-jaw chuck, and insulation was provided between the workpiece and the chuck. The experimental setup, temperature calibration setup, and workpiece material are shown in figure 1, *a*, *b* and *c* respectively. The cutting parameters used for machining are given in Table 2.

Table 1

Chemical composition of work material

Element, %	*SS 316*	*EN 8*	*SAE 8620*	*Al 380*
C	0.07	0.39	0.22	–
Mn	0.16	0.87	0.8	0.5
Si	0.9	0.22	0.28	8.5
P	0.05	0.04	0.031	–
S	0.02	0.05	0.04	–
Cr	18.50	–	0.49	–
Mo	2.25	–	0.22	–
Ni	12.23	–	0.52	0.5
Mg	–	–	–	0.1
Cu	–	–	–	3.6
Sn	–	–	–	0.35
Zn	–	–	–	3
Fe	balance	balance	balance	1.3
Al	–	–	–	balance

a *b* *c*

Fig. 1. Machining Setup (a), Temperature calibration setup (b), Work materials (c)

Table 2

Process parameters and experimental levels

Parameters/Levels	*L 1*	*L 2*	*L 3*	*L 4*	*L 5*
V_c (m/min)	140	190	240	290	340
f (mm/rev)	0.08	0.12	0.16	0.20	0.24
doc (mm)	0.6	0.7	0.8	0.9	1.0

Results and discussion

The central composite design of the response surface method was used for the main experiments. Table 3 shows the experimental results. The objective of the experimental analysis was to identify the significant factor that has a greater influence on the response variables and to develop a generalized empirical model to predict surface roughness and generated temperature using *Buckingham's* $\boldsymbol{\pi}$ theorem. Statistical analysis of surface roughness and temperature rise was carried out using *RSM*.

The main objective of this paper is to develop semi-empirical formulae using the *Levenberg-Marquardt* method to predict the surface roughness and temperature of various materials. Using the values from Table 2, individual regression equations were constructed and the full factorial values were extracted from the regression. These full factorial values are used to derive the semi-empirical formula.

The regression equations for surface roughness of materials are given below.

$$SSR_a = 0.60 + 0.00018V_c + 2.7f - 1.37d - 0.000003V_c^2 + 19.03f +$$

$$0.79d^2 - 0.0050V_c xf + 0.00050V_c xd + 1.87fxd; \tag{I}$$

$$SAER_a = 0.31 - 0.00202V_c + 10.01f - 1.20d - 0.00005V_c^2 + 31c61f^2 -$$

$$0.11d^2 - 0.2604V_c xf + 0.00908V_c xd - 5.1fxd; \tag{II}$$

$$ENR_a = 3.135 - 0.01331V_c - 9.76f - 1.09d + 0.000023V_c^2 + 59.66f^2 +$$

$$0.670d^2 - 0.00312V_c xf + 0.00125V_c xf + 0.31fxd; \tag{III}$$

$$AlR_a = 14.32 - 0.0478V_c - 12.4f - 12.97d + 0.000093V_c^2 + 53.7df^2 +$$

$$7.97d^2 - 0.0444V_c xf - 0.0027V_c xd + 16.6fxd. \tag{IV}$$

Table 3

Experimental data of Ra and temperature for SS 316, EN 8, SAE 8620 and Al 380 materials

Run No.	Speed, V_c, (m/min)	Feed, f, (mm/rev)	**doc**, d, (mm)	*SS 316* R_a	*EN 8* R_a	*SAE 8620* R_a	*AL 380* R_a	*SS 316* Temp	*EN 8* Temp	*SAE 8620* Temp	*Al 380* Temp
1	190	0.12	0.7	0.73	0.84	0.63	2.88	635	636	629	243
2	290	0.12	0.7	0.56	0.66	0.50	1.73	812	657	733	264
3	190	0.2	0.7	1.39	1.54	1.60	3.56	643	654	648	247
4	290	0.2	0.7	1.22	1.31	1.25	2.24	997	672	741	318
5	190	0.12	0.9	0.74	0.92	0.55	2.95	782	647	675	236
6	290	0.12	0.9	0.62	0.74	0.59	1.93	1082	665	782	271
7	190	0.2	0.9	1.47	1.6	1.42	4.08	815	664	735	274
8	290	0.2	0.9	1.27	1.42	1.27	2.52	1157	679	818	334
9	140	0.16	0.8	1.08	1.32	1.12	4.25	732	644	595	229
10	340	0.16	0.8	0.78	1.03	0.80	1.86	1243	689	837	323
11	240	0.08	0.8	0.3	0.59	0.47	2.01	619	629	625	216
12	240	0.24	0.8	1.86	2.06	1.96	2.92	883	666	718	306
13	240	0.16	0.6	0.91	0.92	0.98	2	646	644	693	289
14	240	0.16	1	1.07	1.02	1.04	2.88	1082	653	791	310
15	240	0.16	0.8	1.01	0.95	0.99	2.12	805	649	704	283
16	240	0.16	0.8	0.92	1	0.96	2.24	766	642	694	291
17	240	0.16	0.8	0.93	0.94	1.00	2.31	775	644	699	293
18	240	0.16	0.8	0.99	0.94	1.00	2.09	764	645	701	296
19	240	0.16	0.8	0.96	0.94	1.00	2.1	769	644	703	298
20	240	0.16	0.8	0.98	0.95	1.00	2.08	765	643	701	297

The regression equations for material temperature are given below.

$$SSTemp = 3,517 - 2.74V_c + 696f - 8645d + 0.01054V_c^2 + 3,963f^2 +$$
$$699d^2 + 6.6V_c xf - 1.57V_c xd - 3,281fxd; \quad \text{(V)}$$

$$SAETemp = 1,073 + 0.57V_c + 457f - 1,899d + 0.00210V_c^2 - 3,672f^2 +$$
$$1,175d^2 - 2.14V_c xf - 0.175V_c xd + 2,156fxd; \quad \text{(VI)}$$

$$ENTemp = 748 - 0.787V_c + 87f - 175d + 0.002436V_c^2 + 838d^2 + 159f^2 -$$
$$0.375V_c xf - 0.150V_c xd - 63fxd; \quad \text{(VII)}$$

$$AlTemp = 239 + 0.579V_c + 39f - 353d - 0.001918V_c^2 - 5341d^2 + 108f^2 +$$
$$4.69V_c xf - 0.075V_c xd + 1,344fxd. \quad \text{(VIII)}$$

Buckingham's π theorem

This study uses the dimensional homogeneity principle of *Buckingham's* π theorem [22]. Table 4 shows the mechanical properties of the materials.

Table 4

Units, dimensions and properties of the machined materials

Variable	Unit	Symbol	Dimensions	Workpiece properties			
				SS 316	EN 8	SAE 8620	Al 380
Feed	mm	f	L	–	–	–	–
Speed	m/min	V_c	LT^{-1}	–	–	–	–
Depth of cut	mm	d	L	–	–	–	–
Surface roughness	µm	R_a	L	–	–	–	–
Density	kg/m^3	P	$M L^{-3}$	8,000	7,850	7,845	2,760
Specific Heat	J/kg k	C_p	$L^2 T^{-2} \Theta^{-1}$	0.5	0.475	1.6	0.963
Thermal Conductivity	W/mk	K	$M L T^{-3} \Theta^{-1}$	16.3	46.6	27	109
Yield Strength	N/m^2	σ	$M^{-1} T^{-2}$	240	560	450	159
Coeff. Of Thermal Exp.	m/m×K	α	$L \Theta^{-1}$	16.18×10^{-6}	12.2×10^{-6}	11.6×10^{-6}	12.1×10^{-6}
Temperature	^{o}C	Θ	Θ	1.371	2.600	1.400	650

Quantities of different nature cannot be homogeneous. Applying dimensional analysis, surface roughness can be given by an equation of the following form,

$$R_a = f(F, V, D, \theta, \sigma, K, C_p, \rho, \alpha), \tag{1}$$

where the fundamental dimensions are **ρ**, ***L***, ***T*** and **Θ**. Therefore, since the total number of variables is ten, there are four fundamental dimensions.

The number of dependent and independent variables is $\boldsymbol{n} = 10$, and the number of repeated variables is $\boldsymbol{m} = 4$. Therefore, none of the $\boldsymbol{\pi}$ terms in the present study will be $\boldsymbol{n}–\boldsymbol{m} = 6$.

Thus,

$$f(\pi_1, \pi_2, \pi_3, \pi_4, \pi_5, \pi_6) = 0. \tag{2}$$

Note that equation (2) can also be written as:

$$\pi_1 = f(\pi_1, \pi_2, \pi_3, \pi_4, \pi_5, \pi_6); \tag{3}$$

$$\pi_1 = R_a / F; \tag{4}$$

$$\pi_2 = \left(\frac{C_p \theta}{V^2}\right)^{a_1}; \tag{5}$$

$$\pi_3 = \left(\frac{K\theta}{FV^3 \rho}\right)^{a_2}; \tag{6}$$

$$\pi_4 = \left(\frac{\alpha\theta}{F}\right)^{a_3}; \tag{7}$$

$$\pi_5 = \left(\frac{\sigma}{V^2\rho}\right)^{a_4}; \tag{8}$$

$$\pi_6 = \left(\frac{D}{F}\right)^{a_5}. \tag{9}$$

Therefore, the final form of the equations can be written as

$$R_a = Ø \cdot F\left(\frac{C_p\theta}{V^2}\right)^{a_1}\left(\frac{K\theta}{FV^3\rho}\right)^{a_2}\left(\frac{\alpha\theta}{F}\right)^{a_3}\left(\frac{\sigma}{V^2\rho}\right)^{a_4}\left(\frac{D}{F}\right)^{a_5}. \tag{10}$$

Similarly, the temperature increase (T) can be given by an equation of the following form:

$$\theta = f\left(F, V, \sigma, K, C_p, \rho, \alpha\right); \tag{11}$$

$$\pi_1 = \alpha\theta / F; \tag{12}$$

$$\pi_2 = \left(\frac{FC_p}{\alpha V^2}\right)^{b_1}; \tag{13}$$

$$\pi_3 = \left(\frac{K}{\alpha V^2\rho}\right)^{b_2}; \tag{14}$$

$$\pi_4 = \left(\frac{R_a}{F}\right)^{b_3}; \tag{15}$$

$$\pi_5 = \left(\frac{\sigma}{V^2\rho}\right)^{b_4}; \tag{16}$$

$$\pi_6 = \left(\frac{D}{F}\right)^{b_5}. \tag{17}$$

Thus, the final form of the equation can be written as

$$\theta = F/a \cdot Ø\left(\frac{FC_p}{\alpha V^2}\right)^{b_1}\left(\frac{K}{\alpha V^3\rho}\right)^{b_2}\left(\frac{Ra}{F}\right)^{b_3}\left(\frac{\sigma}{V^2\rho}\right)^{b_4}\left(\frac{D}{F}\right)^{b_5}. \tag{18}$$

Although $\boldsymbol{\alpha}$ appears repeatedly, its' influence on $\boldsymbol{R_a}$ appears to be quite significant. In this work, energy indicators are determined using the *Levenberg-Marquardt* method (see Table 5). The adequacy of the model is further analyzed by comparing the regression of $\boldsymbol{R_a}$ and the predicted values of the semi-empirical model.

Table 5

Coefficients and energy indicators of $\boldsymbol{R_a}$ and temperature model

Energy indicators	Surface roughness	Energy indicators	Temperature
Ø	1.687688	**Ø**	0.098376
$\boldsymbol{a_1}$	0.118057	$\boldsymbol{b_1}$	–0.186434
$\boldsymbol{a_2}$	0.322659	$\boldsymbol{b_2}$	–0.384552
$\boldsymbol{a_3}$	–0.591654	$\boldsymbol{b_3}$	–0.177437
$\boldsymbol{a_4}$	–0.272547	$\boldsymbol{b_4}$	0.407445
$\boldsymbol{a_5}$	0.548434	$\boldsymbol{b_5}$	0.660121

Comparison of surface roughness of *SS 316*, *EN 8*, *SAE 8620* and *Al 380*

To obtain a complete understanding of the influence of input parameters on surface roughness, three-dimensional (3D) surface diagrams were constructed for all cutting materials by varying process parameters. These visual representations use empirically derived equations to ensure accuracy. Figure 2 shows three-dimensional surface diagrams illustrating the surface roughness changes during turning of *SS 316*, *EN 8*, *SAE 8620* and *Al 380* with *PVD*-coated (*TiAlN*) tools generated using Eqs. (I)–(IV).

From figure 2 it becomes clear that the surface roughness is primarily affected by the feed. However, this effect can be considered to be more significant for *Al 380* and *SS 316*. During the processing of aluminum alloys, built-up edges are formed due to the adhesion of chips to the cutting tool, which leads to an increase in surface roughness. In the case of *SS 316*, there is a tendency for the formation of drain chips that spin around the work material, damaging the new surface, and this may be the cause of poor surface finish. *EN 8* and *SAE 8620* materials seem well suited for machining, mainly due to their low hot hardness and easy machinability. Therefore, the roughness of these materials is higher compared to others. It was also observed that as cutting speed increases, there is a tendency for surface roughness to improve for all materials. The literature reports that at high cutting speeds, the tool-chip contact length is reduced, thereby minimizing cutting tool vibration and improving surface roughness. In addition, at higher speeds, the cutting temperature increases; this contributes to the softening of the material. This in turn helps reduce cutting forces, thereby minimizing vibration and improving surface finish.

Figure 3, *a* shows the effect of $\boldsymbol{f}$ on $\boldsymbol{R_a}$ at $\boldsymbol{V_c}$ = 140 m/min and ***doc*** = 0.6 mm for both regression and semi-empirical values. Aluminum material has poor surface finish because aluminum produces more continuous chips than other materials. In addition, this continuous chip damages the finished parts [23].

Figure 3, *b* shows the effect of f on $\boldsymbol{R_a}$ at $\boldsymbol{V_c}$ = 190 m/min and ***doc*** = 0.7 mm. As f increases, $\boldsymbol{R_a}$ increases compared to other materials, the thermal conductivity of *SS 316* is lower, due to the increase in temperature,

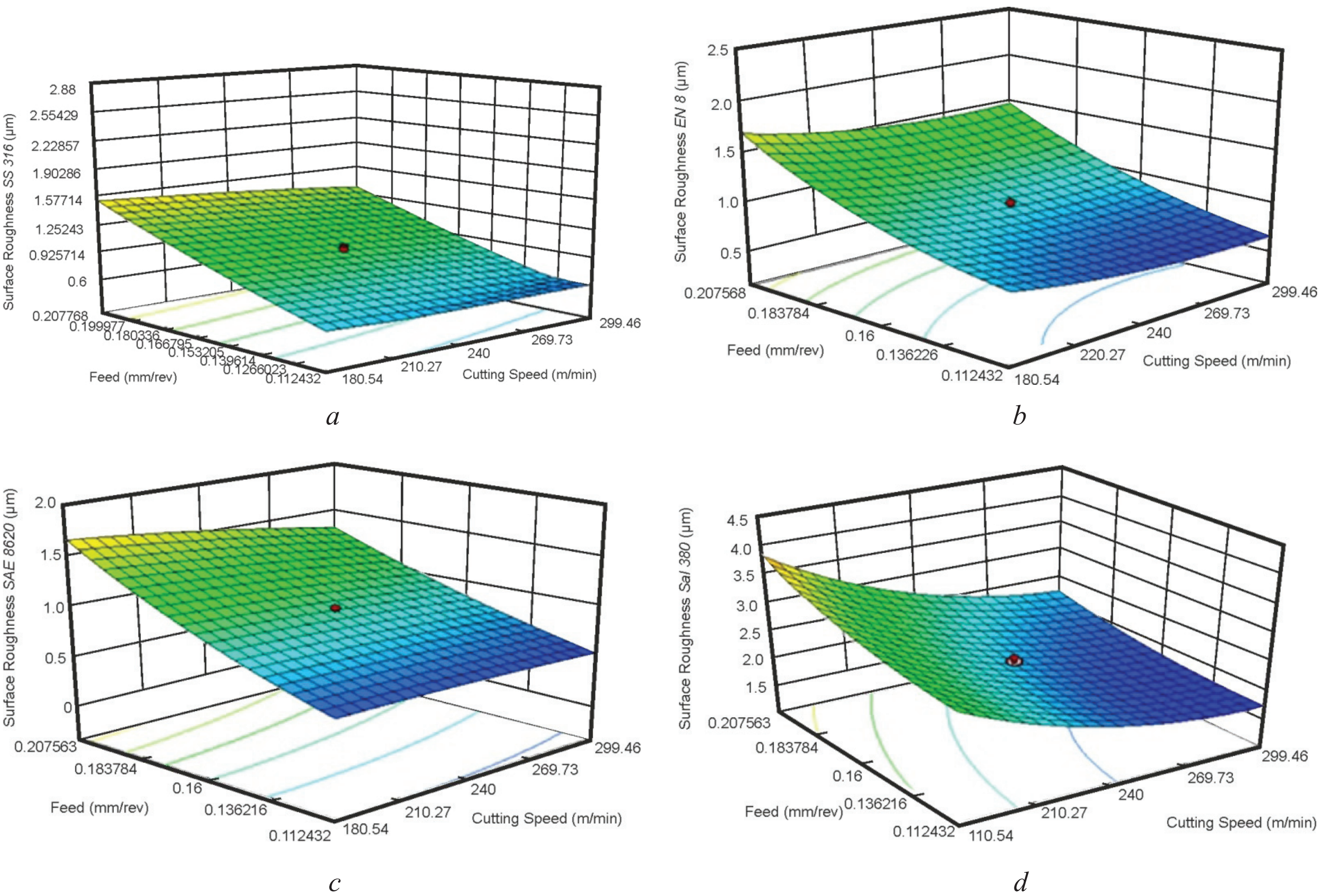

Fig. 2. Surface roughness 3D-plots for *SS 316* (*a*), *EN 8* (*b*), *SAE 8620* (*c*) and *Al 380* (*d*)

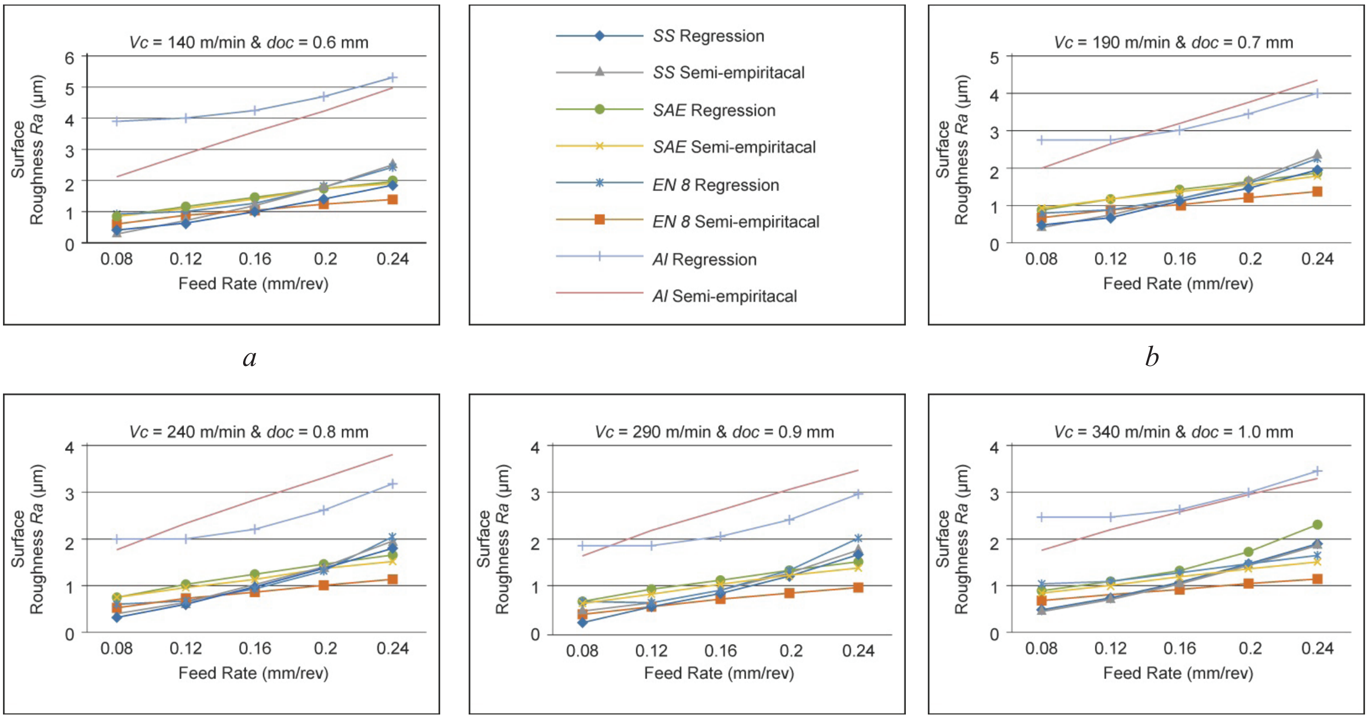

a *b*

c *d* *e*

Fig. 3. Effect of feed rate on surface roughness at different cutting speed and depth of cut for all materials using *TiAlN*-coated tool

the material becomes more ductile when cutting and a smoother cut is possible, which leads to better surface quality [11]. The minimum $\boldsymbol{R_a}$ is achieved by increasing $\boldsymbol{V_c}$ from 240 m/min to 340 m/min and ***doc*** from 0.8 mm to 1 mm, as shown in figure 3 c–e, since at higher $\boldsymbol{V_c}$ the strain rate in the shear zone is expected to be high, which will lead to an increase in temperature [2]. As $\boldsymbol{V_c}$ and f increase, the temperature increases because the heat dissipation time decreases and the larger chip-tool contact area increases friction. $\boldsymbol{V_c}$ and ***doc*** are significant factors in increasing tool temperature for *SS 316* and *SAE 8620*. $\boldsymbol{R_a}$ decreases due to increasing strain rate [24].

Figure 4, *a–e* clearly shows that higher ***Vc*** provides good surface roughness for almost all materials. However, as ***f*** and ***doc*** increase, the surface roughness increases first for *SS 316* and then for *Al 380*. *EN 8* shows even better results due to low heat generation in the cutting zone, which maintains tool shape stability. Since the thermal conductivity of *SS 316* is lower compared to other materials, it becomes more ductile during cutting due to increased temperature, and a smoother cut is possible due to better surface quality [2]. $\boldsymbol{R_a}$ was found to be the worst when machining *Al 380* and was superior to *SS 316* and *SAE 8620*. The sticking of *Al 380* material results in a rough surface. Built-up edge occurs because the material easily adheres to the cutting edge, which ultimately changes the geometry of the tool and ***Ra*** increases [12].

Figure 5 a–e shows the effect of ***doc*** on various materials. It is observed that ***doc*** does not have a significant effect on $\boldsymbol{R_a}$. This may be due to the increase in strain volume with increasing ***doc***. Thus, severe deformation of the workpiece results in more surface irregularities and hence poor surface quality. *Zou et al.* [25] also obtained similar results. ***Doc*** is less significant for ***Ra*** than ***Vc*** and ***f*** [11]. At higher values of technological parameters, the thermal wear of the tool and surface roughness increase [3].

Comparison of cutting temperatures of SS 316, EN 8, SAE 8620 and Al 380

To obtain a comprehensive understanding of the influence of input parameters on cutting temperature, three-dimensional (3-D) surface plots are constructed by varying the process parameters for all cutting materials. These visual representations use empirically derived equations to ensure accuracy. Figure 6 shows three-dimensional diagrams illustrating the cutting temperature changes during turning of *SS 316*, *EN 8*, *SAE 8620* and *Al 380* stainless steels for *PVD*-coated (*TiAlN*) tools obtained using equations (V)–(VIII).

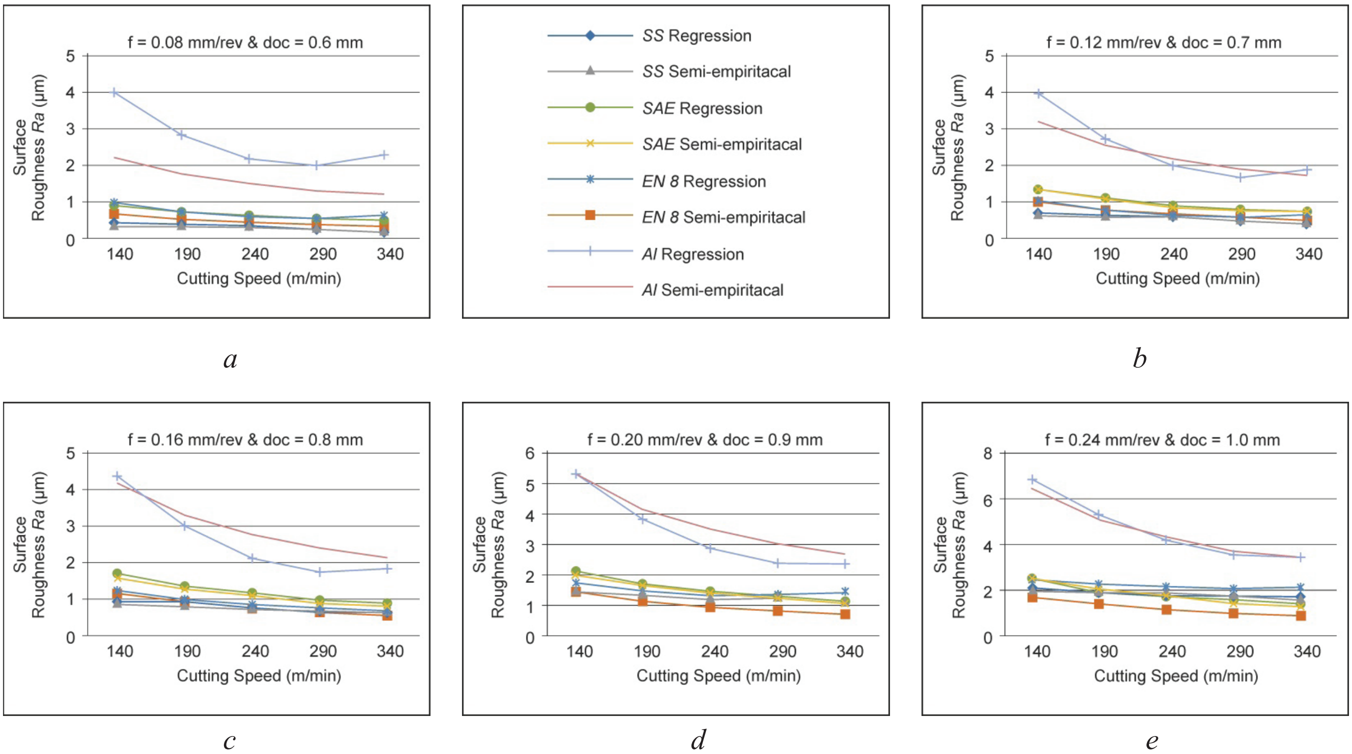

Fig. 4. Effect of cutting speed on surface roughness at different feed rate and depth of cut for all materials using *TiAlN*-coated tool

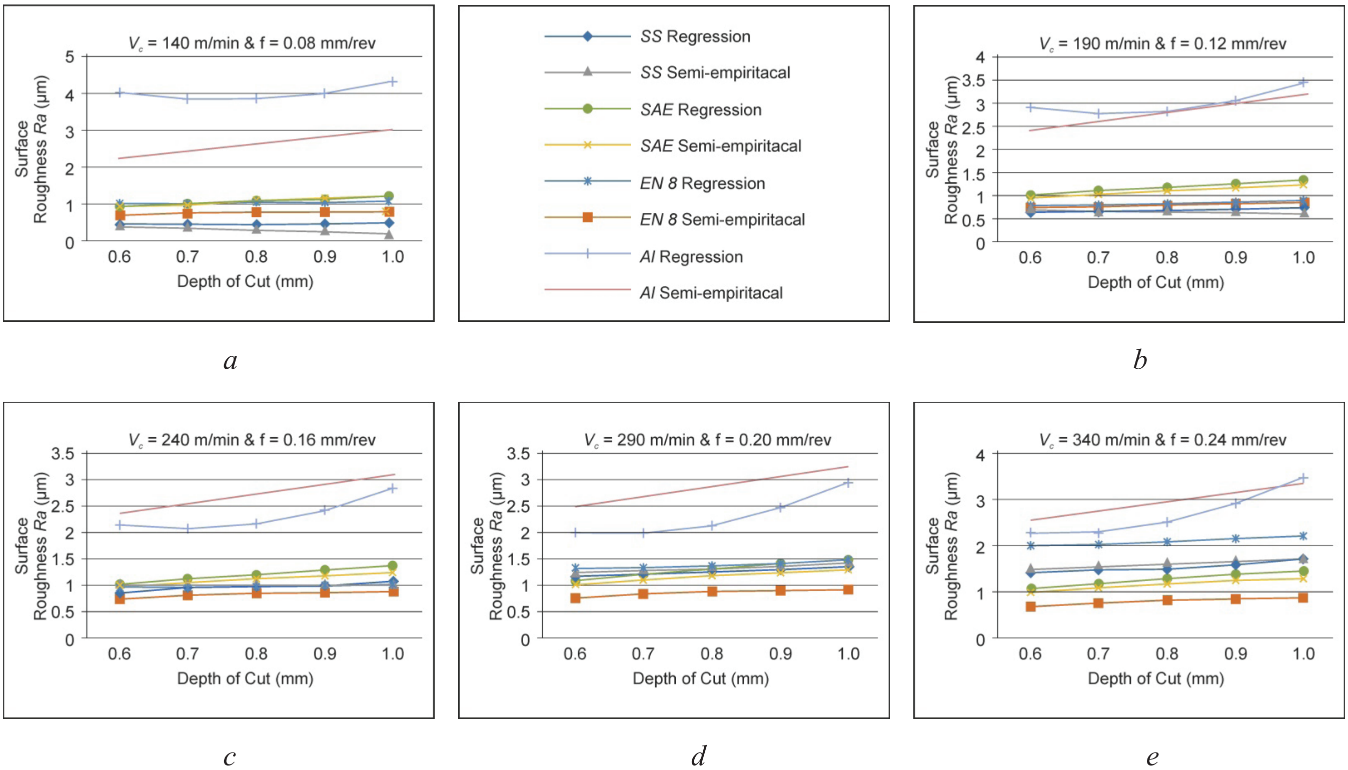

Fig. 5. Effect of depth of cut on surface roughness at different feed rate and cutting speed for all materials using *TiAlN*-coated tool

In the case of cutting temperature, ***f*** does not have a significant effect (see figure 6, *a–d*). Compared to other materials, *Al 380* exhibits a less significant temperature increase. In other materials such as *SS 316*, *SAE 380* and *EN 8*, the temperature rise is linear, low thermal conductivity and specific heat capacity are responsible for the large variations in temperature rise in *SS 316*. Consequently, the temperature during

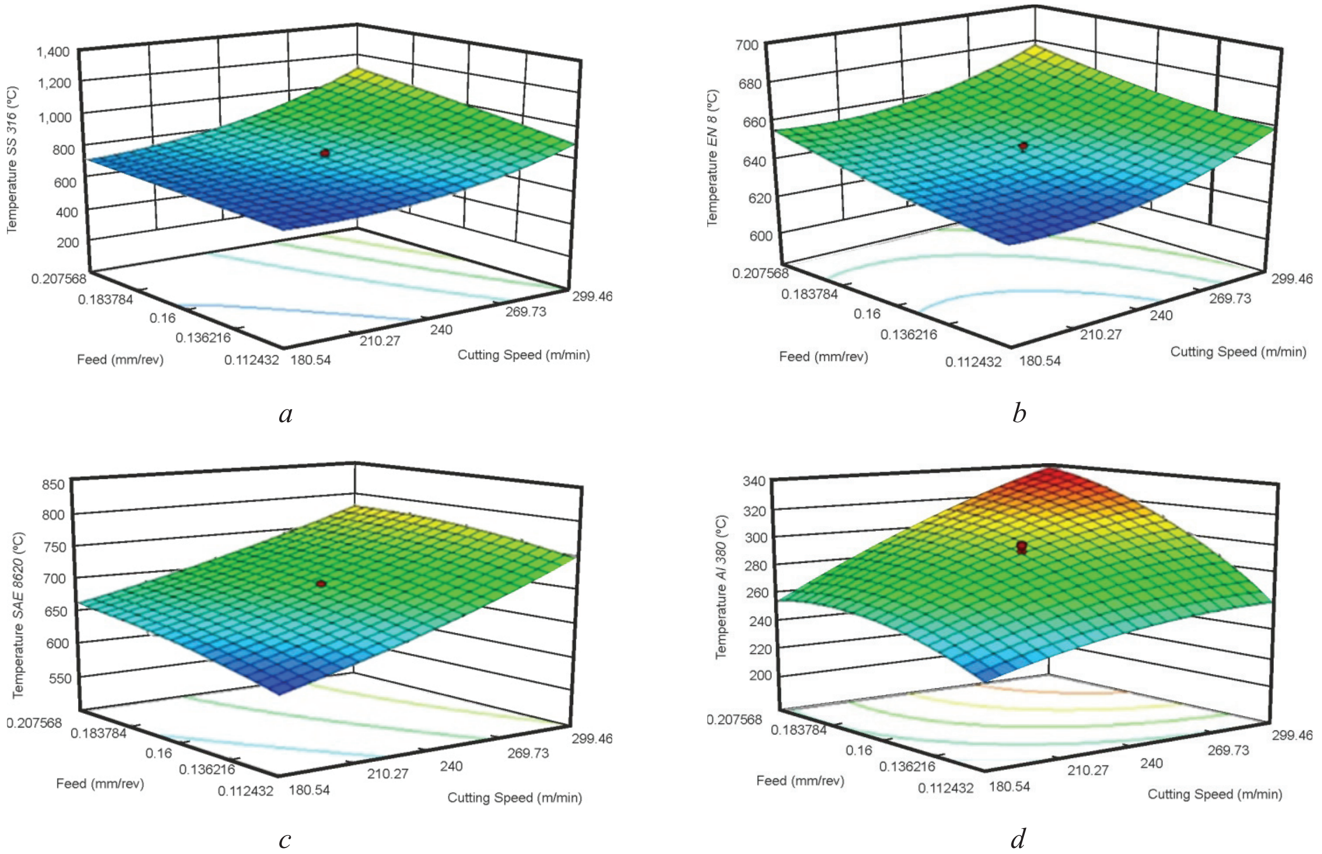

Fig. 6. Cutting temperature 3D-plots for *SS 316* (*a*), *EN 8* (*b*), *SAE 8620* (*c*) and *Al 380* (*d*)

processing of *SS 316* increases as the process parameters increase. High-speed, high-temperature processing results were obtained with increasing V_c. Most of the heat is carried away by the chips, and little heat is lost into the workpiece. It can be seen that f affects the temperature slightly, but gradually the temperature continues to increase as f increases. The same result was obtained by *Dessoly et al.* [26] using a *FEM* model and an *IR* camera. Figure 7 a, b shows that with increasing f the temperature increases, since a larger surface area of the workpiece and the tool is in contact. Aluminum has the lowest yield strength, so heat generation in aluminum is less compared to other materials.

Figure 7, *c–e* shows how the temperature increases with increasing f, ***doc***, and V_c increases. Increasing f increases the temperature due to greater chip-tool contact and associated friction [27]. In aluminum, the temperature rises to a lesser extent because due to higher thermal conductivity, heat transfer occurs faster, so the material remains in the same state throughout, the material does not become more ductile, and the friction between the workpiece and the cutting tool is reduced [12]. As the process parameters increase, the temperature increases. *Kitagawa et al.* [28] used ceramic tools to turn *Inconel 718* and found that the cutting temperature continued to increase with increasing process parameters as the workpiece material was deformed into chips by the cutting tools. Deformation of the workpiece, cohesion or friction of the chips on the rake surface of the tool leads to strong heating [3].

As V_c increases, the temperature continues to rise. As a result, the surface quality decreases and tool wear increases [1]. In figure 8 cutting temperature is directly proportional to cutting speed. However, it also depends on other factors such as f, ***doc***, cutting width, machine operating conditions [27]. Figure 8, *a–e* shows the effect of ***doc*** on cutting temperature. The temperature continues to increase with increasing ***doc*** because at maximum feed and ***doc***, large frictional heat is generated due to the friction between the work material and the cutting tool, which leads to thermal softening of the material [29]. According to semi-empirical and regression results, ***doc*** is a more significant temperature parameter than f and V_c [1].

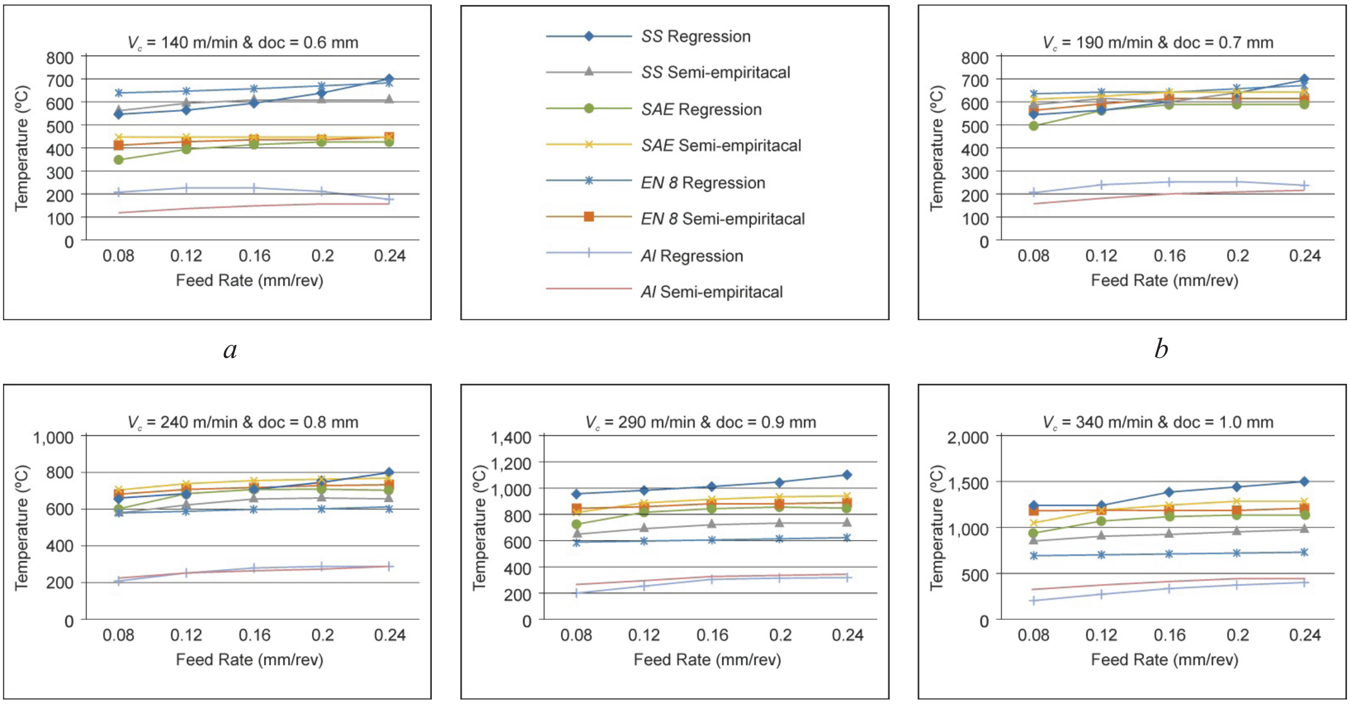

a *b*

c *d* *e*

Fig. 7. Effect of feed rate on cutting temperature at different cutting speed and depth of cut for all materials using *TiAlN*-coated tool

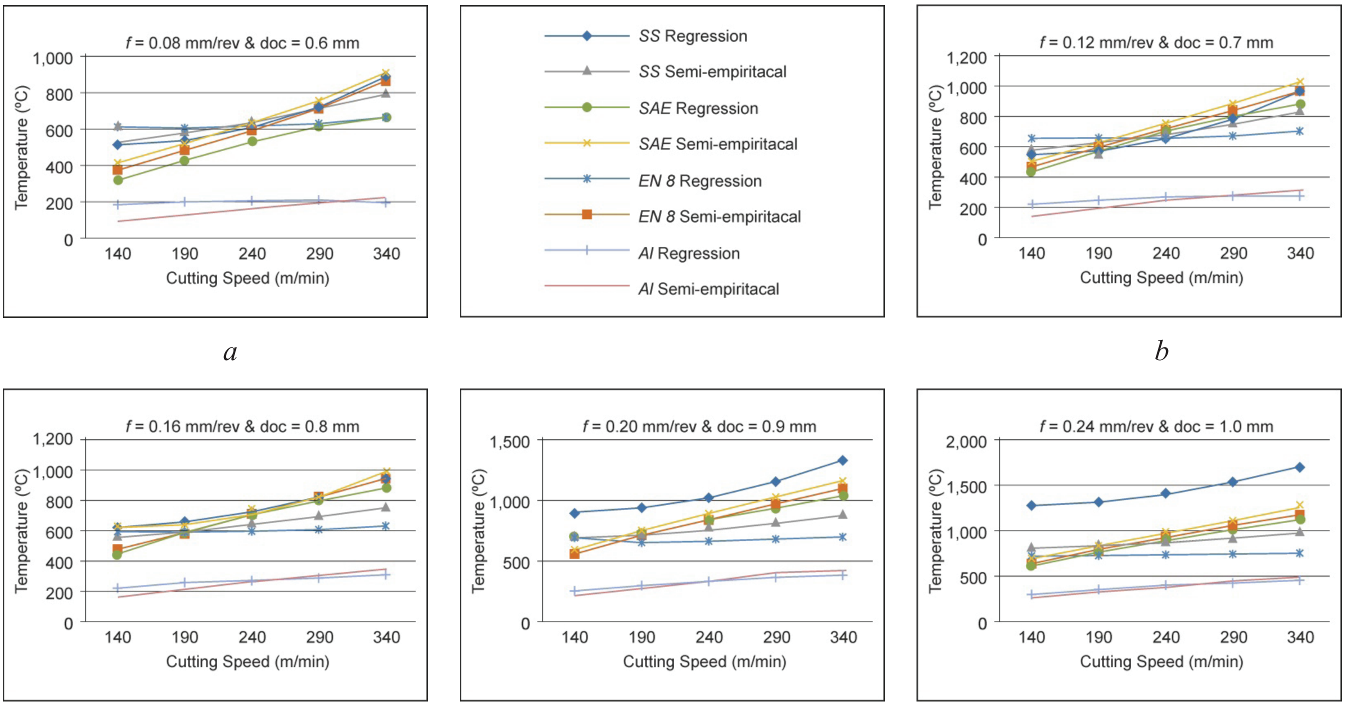

a *b*

c *d* *e*

Fig. 8. Effect of cutting speed on cutting temperature at different feed rate and depth of cut for all material using *TiAlN*-coated tool

In figure 9, *a–e* the workpiece or tool is enlarged due to the heat generated. Cutting temperature greatly influences the mechanical properties of the workpiece and the forces acting on the workpiece and tool [30]. Most of the total heat is transferred to the chip, and this total heat in the chip flow is due to shear and friction at the chip-tool interface. Changing ***doc*** has a greater impact on the cutting temperature compared to $\boldsymbol{f}$ and $\boldsymbol{V_c}$ [8].

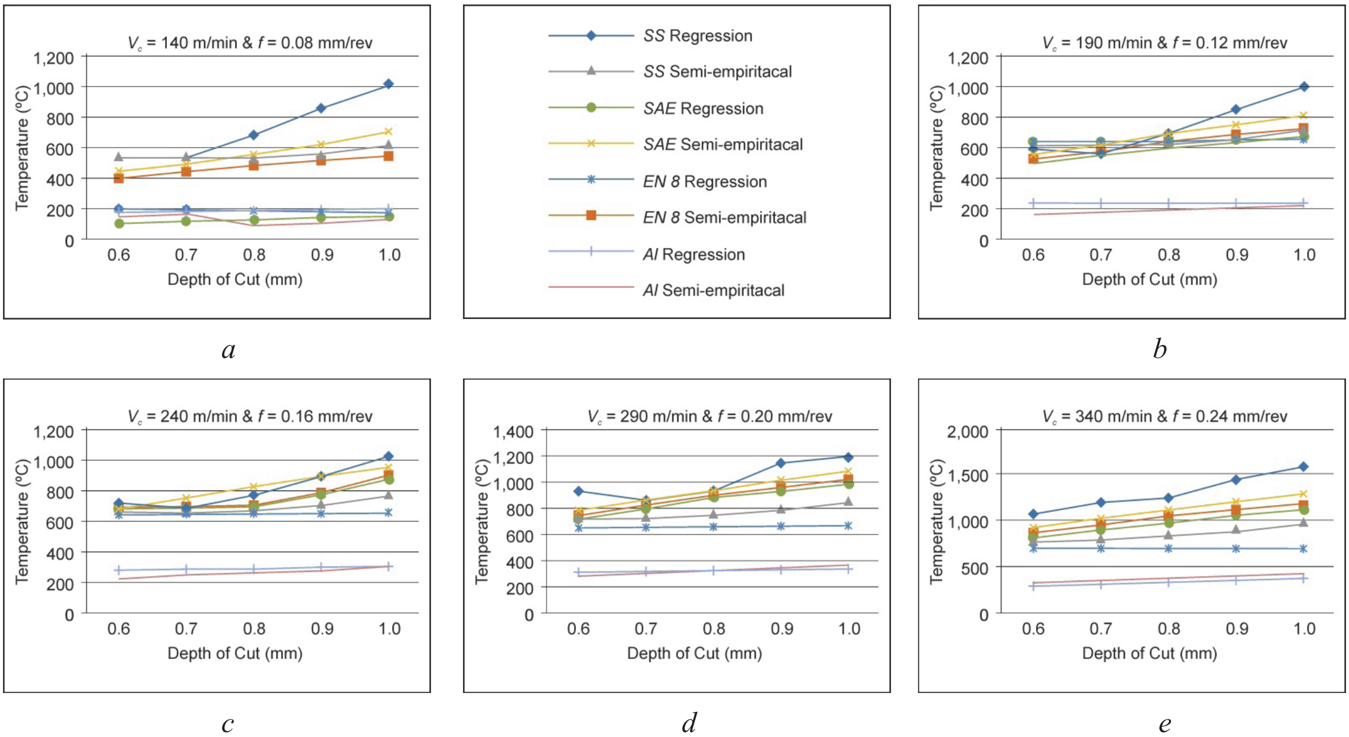

Fig. 9. Effect of depth of cut on cutting temperature at different feed rate and cutting speed for all material using *TiAlN*-coated tool

All figures show the results of regression values taken from the empirical model and experimental *RSM* values for temperature and surface roughness, which were found to be comparable. All values of the *RSM* output parameters and the empirical model values are in good agreement with each other. Therefore, Equations (10) and (18) can be used to determine the theoretical value of $\boldsymbol{R_a}$ and temperature at different cutting parameters for different work materials with *TiAlN*-coated carbide tool inserts.

Conclusions

A semi-empirical method, taking into account the dimensions of material properties, is proposed for estimating cutting temperature and surface roughness when turning *SS 316*, *SAE 8620*, *EN 8* and *Al 380* workpieces with *PVD*-coated carbide (*TiAlN*) inserts. In addition, a multilinear regression analysis was carried out and based on the analysis of the results of the regression and semi-empirical model, the following conclusions were drawn:

● At higher feed rates, low surface roughness is observed for all materials. However, as feed and depth of cut increase, surface roughness tends to increase more in *SS 316*, then *Al 380*. *EN 8* shows better results due to low heat generation in the cutting zone, which maintains tool shape stability.

● The rapid work hardening of the chips in the case of *SS 316*, the toughness of the chip and built-up material, the stability of the tool shape in the case of *EN 8* and *SAE 8620* are the main reasons for the surface roughness quality.

● Higher cutting temperature is obtained when turning *SS 316* and lower cutting temperature is obtained when turning *Al 380*. This is due to the significant difference in thermal conductivity of these materials.

● When machining *EN 8* and *SAE 8620*, the cutting temperature range is found to be moderate.

● Surface roughness is found to be worst for *Al 380* and best for *SS 316* and *SAE 8620*.

● In addition, using a dimensional analysis model, a generalized empirical formula is developed to predict the surface roughness and temperature encountered during metal cutting. These models are found to fit well with regression equations derived from experimental values.

● The proposed method for measuring surface roughness and temperature can be conveniently used. This is a useful way to cost-effectively evaluate heat generation and surface roughness when turning various materials with *TiAlN*-coated carbide tools.

References

1. Ghosh P.S., Chakraborty S., Biswas A.R., Mandal N.K. Empirical modelling and optimization of temperature and machine vibration in CNC hard turning. *Materials Today: Proceedings*, 2018, vol. 5 (5), pp. 2394–12402. DOI: 10.1016/j.matpr.2018.02.218.

2. Groover M.P. *Fundamentals of modern manufacturing: materials, processes, and systems*. 4th ed. Hoboken, NJ, Wiley, 2010. 1012 p. ISBN 978-0470-467002.

3. Zhao J., Liu Z., Wang B., Hua Y., Wang Q. Cutting temperature measurement using an improved two-color infrared thermometer in turning Inconel 718 with whisker-reinforced ceramic tools. *Ceramics International*, 2018, vol. 44 (15), pp. 19002–19007. DOI: 10.1016/j.ceramint.2018.07.142.

4. Kakade H.B., Patil N.G. Comparative investigations into high speed machining of AB titanium alloy (Ti–6al–4v) under dry and compressed Co_2 gas cooling environment. *AIP Conference Proceedings*, 2018, vol. 2018 (1), pp. 20009-1–20009-9. DOI: 10.1063/1.5058246.

5. Gunjal S.U., Sanap S.B., Patil N.G. Role of cutting fluids under minimum quantity lubrication: an experimental investigation of chip thickness. *Materials Today: Proceedings*, 2020, vol. 28 (2), pp. 1101–1105. DOI: 10.1016/j.matpr.2020.01.090.

6. Kulkarni A.P., Chinchanikar S., Sargade V.G. Dimensional analysis and ANN simulation of chip-tool interface temperature during turning SS304. *Obrabotka metallov (tekhnologiya, oborudovanie, instrumenty) = Metal Working and Material Science*, 2021, vol. 23, no. 4, pp. 47–64. DOI: 10.17212/1994-6309-2021-23.4-47-64. (In Russian).

7. Kumar R., Sahoo A.K., Das R.K., Panda A., Mishra P.C. Modelling of flank wear, surface roughness and cutting temperature in sustainable hard turning of AISI D2 steel. *Procedia Manufacturing*, 2018, vol. 20, pp. 406–413. DOI: 10.1016/j.promfg.2018.02.059.

8. Gosai M., Bhavsar S.N. Experimental study on temperature measurement in turning operation of hardened steel (EN36). *Procedia Technology*, 2016, vol. 23, pp. 311–318. DOI: 10.1016/j.protcy.2016.03.032.

9. Abhang L.B., Hameedullah M. Chip-tool interface temperature prediction model for turning process. *International Journal of Engineering Science and Technology*, 2010, vol. 2 (4), pp. 382–393.

10. Doniavi A., Eskanderzade M., Tahmsebian M. Empirical modeling of surface roughness in turning process of 1060 steel using factorial design methodology. *Journal of Applied Sciences*, 2007, vol. 7 (17), pp. 2509–2513. DOI: 10.3923/jas.2007.2509.2513.

11. Verma V., Kumar J., Singh A. Optimization of material removal rate and surface roughness in turning of 316 steel by using full factorial method. *Materials Today: Proceedings*, 2020, vol. 25, pp. 793–798. DOI: 10.1016/j.matpr.2019.09.029.

12. Das D., Ali R.F., Nayak B.B., Routara B.C. Investigation on surface roughness and chip reduction coefficient during turning aluminium matrix composite. *Materials Today: Proceedings*, 2019, vol. 5 (11), pp. 23541–23548. DOI: 10.1016/j.matpr.2018.10.142.

13. Bhople N., Patil N., Mastud S. The experimental investigations into dry turning of austempered ductile iron. *Procedia Manufacturing*, 2018, vol. 20, pp. 227–232. DOI: 10.1016/j.promfg.2018.02.033.

14. Aouici H., Yallese M.A., Chaoui K., Mabrouki T., Rigal J.F. Analysis of surface roughness and cutting force components in hard turning with CBN tool: prediction model and cutting conditions optimization. *Measurement*, 2012, vol. 45 (3), pp. 344–353. DOI: 10.1016/j.measurement.2011.11.011.

15. Longbottom J.M., Lanham J.D. Cutting temperature measurement while machining – a review. *Aircraft Engineering and Aerospace Technology*, 2005, vol. 77 (2), pp. 122–130. DOI: 10.1108/00022660510585956.

16. Korkut I., Acır A., Boy M. Application of regression and artificial neural network analysis in modelling of tool–chip interface temperature in machining. *Expert Systems with Applications*, 2011, vol. 38 (9), pp. 11651–11656. DOI: 10.1016/j.eswa.2011.03.044.

17. Dhar N.R., Kamruzzaman M. Cutting temperature, tool wear, surface roughness and dimensional deviation in turning AISI-4037 steel under cryogenic condition. *International Journal of Machine Tools and Manufacture*, 2007, vol. 47 (5), pp. 754–759. DOI: 10.1016/j.ijmachtools.2006.09.018.

18. Patil N.G., Brahmankar P.K. Semi-empirical modeling of surface roughness in wire electro-discharge machining of ceramic particulate reinforced Al matrix composites. *Procedia CIRP*, 2016, vol. 42, pp. 280–285. DOI: 10.1016/j.procir.2016.02.286.

19. Patel D.R., Kiran M.B. A non-contact approach for surface roughness prediction in CNC turning using a linear regression model. *Materials Today: Proceedings*, 2020, vol. 26, pp. 350–355. DOI: 10.1016/j.matpr.2019.12.029.

20. Patel V.D., Gandhi A.H. Analysis and modeling of surface roughness based on cutting parameters and tool nose radius in turning of AISI D2 steel using CBN tool. *Measurement*, 2019, vol. 138, pp. 34–38. DOI: 10.1016/j.measurement.2019.01.077.

21. Rodríguez J., Munoz-Escalona P., Cassier Z. Influence of cutting parameters and material properties on cutting temperature when turning stainless steel. *Revista de la Facultad de Ingeniería Universidad Central de Venezuela*, 2011, vol. 26 (1), pp. 71–80.

22. Rajput R.K. *A textbook of fluid mechanics and hydraulic machines*. New Delhi, S. Chand, 2004. ISBN 9789385401374.

23. Saravanakumar A., Karthikeyan S.C., Dhamotharan B., Gokul kumar V. Optimization of CNC turning parameters on aluminum alloy 6063 using Taguchi Robust Design. *Materials Today: Proceedings*, 2018, vol. 5 (2), pp. 8290–8298. DOI: 10.1016/j.matpr.2017.11.520.

24. Smith W.F. *Structure and properties of engineering alloys*. New York, McGraw-Hill, 1981. 512 p. ISBN 0070585601. ISBN 978-0070585607.

25. Zou B., Chen M., Li S. Study on finish-turning of NiCr20TiAl nickel-based alloy using Al_2O_3/TiN-coated carbide tools. *The International Journal of Advanced Manufacturing Technology*, 2011, vol. 53 (1), pp. 81–92. DOI: 10.1007/s00170-010-2823-z.

26. Dessoly V., Melkote S.N., Lescalier C. Modeling and verification of cutting tool temperatures in rotary tool turning of hardened steel. *International Journal of Machine Tools and Manufacture*, 2004, vol. 44 (14), pp. 1463–1470. DOI: 10.1016/j.ijmachtools.2004.05.007.

27. Rezende B.A., Magalhaes F.C., Rubio J.C.C. Study of the measurement and mathematical modelling of temperature in turning by means equivalent thermal conductivity. *Measurement*, 2020, vol. 152, pp. 107275. DOI: 10.1016/j.measurement.2019.107275.

28. Kitagawa T., Kubo A., Maekawa K. Temperature and wear of cutting tools in high-speed machining of Inconel 718 and Ti–6Al–6V–2Sn. *Wear*, 1997, vol. 202 (2), pp. 142–148. DOI: 10.1016/S0043-1648(96)07255-9.

29. Pawade R.S., Joshi S.S. Analysis of acoustic emission signals and surface integrity in the high-speed turning of Inconel 718. *Proceedings of the Institution of Mechanical Engineers, Part B: Journal of Engineering Manufacture*, 2012, vol. 226 (1), pp. 3–27. DOI: 10.1177/0954405411407656.

30. Aydın M., Karakuzu C., Uçar M., Cengiz A., Çavuşlu M.A. Prediction of surface roughness and cutting zone temperature in dry turning processes of AISI304 stainless steel using ANFIS with PSO learning. *The International Journal of Advanced Manufacturing Technology*, 2013, vol. 67 (1), pp. 957–967. DOI: 10.1007/s00170-012-4540-2.

Conflicts of Interest

The authors declare no conflict of interest.